Structural Eng./Earthquake Eng. Vol. 8, No. 2, 75s-85s, July 1991
Japan Society of Civil Engineers (Proc. of JSCE No. 432/I-16)

APPLICATION OF THE DISTINCT ELEMENT METHOD TO THE NUMERICAL ANALYSIS OF DEBRIS FLOWS

Motohiko HAKUNO*
and Yoshihiko UCHIDA**

Slope slides, dry rock avalanches and debris flows frequently take place in mountainous areas following strong earthquakes. Various types of flow analysis have been made based on a continuous medium. But, as the rocks and soil which are contained in rock avalanches and debris flows, are discontinuous not continuous materials. We have developed a modification of Distinct Element Method in which the effect of water present between particles is taken into account. By using the extended DEM for debris flows, we could follow their flow processes and compare them with those of the dry rock avalanches. In addition, we obtained simulation results that explain the flow behaviors when the flow makes an impact with dam wall and the deposition process.

Keywords : *distinct element method, debris flow*

1. INTRODUCTION

Landslides and rock avalanches frequently occur after strong earthquakes in mountainous regions, as in the example of the Western Nagano Earthquake of 1984. The landslide of the earthquake flows as a rock avalanche that has little moisture during the initial stage of collapse but obtains water content from outside downstream and in many cases becomes a debris flow with much water.

We analyzed debris flows using a method that is based on the Distinct Element Method (DEM)[3)-8)] originated by Cundall, in which an equation of motion is formulated for each particle, after which an aggregate of particles is analyzed instead of using the method for the theoretical analysis of granular matter[1),2)]. We also investigated the flow situation on irregular slopes and made numerical simulations of the behavior and impact pressure when a debris flow collides with a vertical wall, such as a sediment control dam (sabo dam), as well as making a simulation of the deposition process after the debris flow reaches a levee area.

2. EQUATION OF MOTION FOR ROCK PARTICLES

The DEM is a method for analyzing granular material. In a two-dimensional case the following equations of motion (1) and (2) are derived :

$$m_i d^2V/dt^2 + C_i dV/dt + F_i = 0 \quad \cdots\cdots (1)$$

and

$$I_i d^2\phi/dt^2 + D_i d\phi/dt + M_i = 0 \quad \cdots\cdots (2)$$

* Earthquake Research Institute, University of Tokyo (Yayoi 1-1-1, Bunkyou-ku, Tokyo)
** Central Japan Railway Company

where F_i:resultant force acting on the i-th particle, M_i:resultant moment acting on the i-th particle, C_i and D_i:respective damping coefficients for to translation and rotation, which are specified as caused by the internal friction and air resistance on particles, V:displacement vector, ϕ:rotation angle, m_i:mass of the i-th particle, I_i:moment of inertia of the i-th particle. In the preceding equations the resultant forces and moments are derived from the deformations of two springs inserted either normally or tangentially between the relevant particles (**Fig.1**). These springs naturally have such nonlinear characteristics as loss of resistance under tension in the normal direction or slip over a limited friction force in the tangential direction. Therefore, the only unknowns in (1) and (2) are V and ϕ, which are obtained by convering the relations to finite difference equations and by integrating them respect to time in the forward direction.

The conventional distinct element method could not be used because the particles in a debris flow are saturated with water. Saturation hsd been considered in examples of liquefaction problem, but the number of calculations became too great, and it was not possible to make calculations for the period of time (10 to 20 seconds) experienced in real phenomena.

Therefore, in this analysis we have used a mutual interference terms, the f_n, f_s with water as the medium that is proportional to the square of the relative velocity of the particles. Also, acting direction of f_n, f_s was established as the repulsive direction when particles are approaching and to be the opposing direction when they oppose.

$$[f_n]_t = C_D a \rho_\omega [V_n]_t^2/2 \quad \cdots\cdots (3)$$

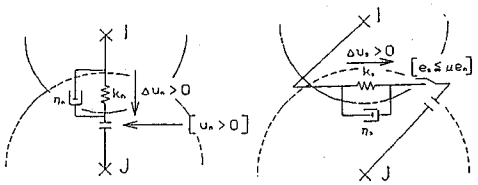

Fig.1 Mechanical model at contact point.

Table 1 Parameters used in simulation.

K_n	9.0×10^6	(N/m)
K_s	3.0×10^6	(N/m)
η_n	2.0×10^3	(N sec/m)
η_s	1.0×10^3	(N sec/m)
ρ_s	2.5×10^3	(kg/m³)
ρ_w	1.5×10^3	(kg/m³)
$\triangle t$	2.5×10^{-4}	(sec)
e	0.05	
μ	0.1	
C_D	0.70	Radius<0.50m
	0.66	0.50m<Radius<0.75m
	0.60	0.75m<Radius

Table 2 Mechanical parameters of a particle.

K_n	Normal spring constant of particle (N/m)
K_s	Shear spring constant of particle (N/m)
η_n	Normal damping coefficient (N sec/m)
η_s	Transverse damping coefficient (N sec/m)
ρ_s	Density of particle (Kg/m³)
ρ_w	Density of water (Kg/m³)
$\triangle t$	Time step for computation (sec)
e	Restitution coefficient
μ	Friction coefficient
C_D	Water resistance coefficent of particle

$$[f_s]_t = C_D a \rho_\omega [V_s]_t^2/2 \quad \cdots\cdots (4)$$

where, f: Resisting force to particles.
v: Relative velocity of particles.
Subscripts n, s: Components in the normal and tangential directions.
C_D: Drag coefficient.
a: Projected area of particle in its flow direction.
ρ_ω: Density of water.

The parameters C_D, K_n, K_s, etc. adopted in the actual numerical calculations are shown in **Tables 1** and **2**.

3. FLOW-DOWN SITUATION ON ROUGH SLOPES

As the round granular assembly that flows down a slope, the compacted granular assembly model

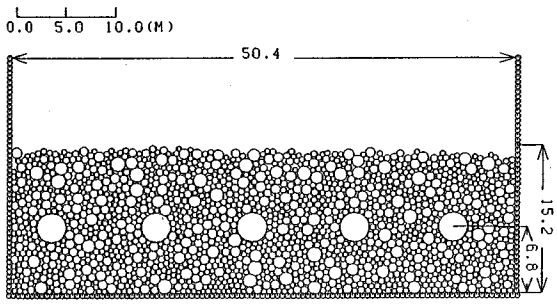

Fig.2 Granular assembly model after compaction.

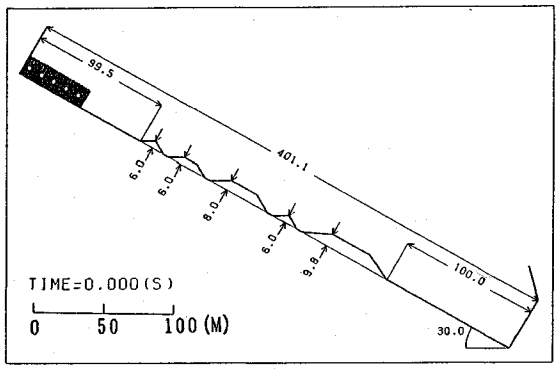

Fig.3 Rough slope [Unit: Length (m)・Angle (Degree)]

shown in **Fig.2** was used. It was made by compacting 1 000 two-dimensional round particles with grain sizes of logarithmic normal distribution. Five large particles also were distributed (**Fig.2**). This model was placed at the upstream end on the left side of a rough slope with a gradient of 30° (**Fig.3**). The flow of the model down the slope was by acceleration due to gravity only. Results are shown in **Fig.4 (a)**.

Results of a dry granular rock avalanche for which the influence of water was not considered are shown in **Fig.4 (b)**. These are compared with results of a debris flow for the same elapsed time after the start of calculation. This figure shows that the characteristics of a debris flow is that there is little scattering compared to a granular rock avalanche and its flow-down velocity is relatively low.

The mean velocity distribution from the botom surface to the flow surface in a cross section perpendicular to the direction of debris flow is shown in **Fig.5**, and **Fig.6** shows a similar distribution for a granular rock avalanche. A comparison of both velocity distributions shows that their shapes are similar, but the scale of the abscissa indicates a slower overall velocity for the debris flow. Stage 5 in **Fig.5** indicates a very low velocity for the portion close to the slope as compared to the other portions. This is because

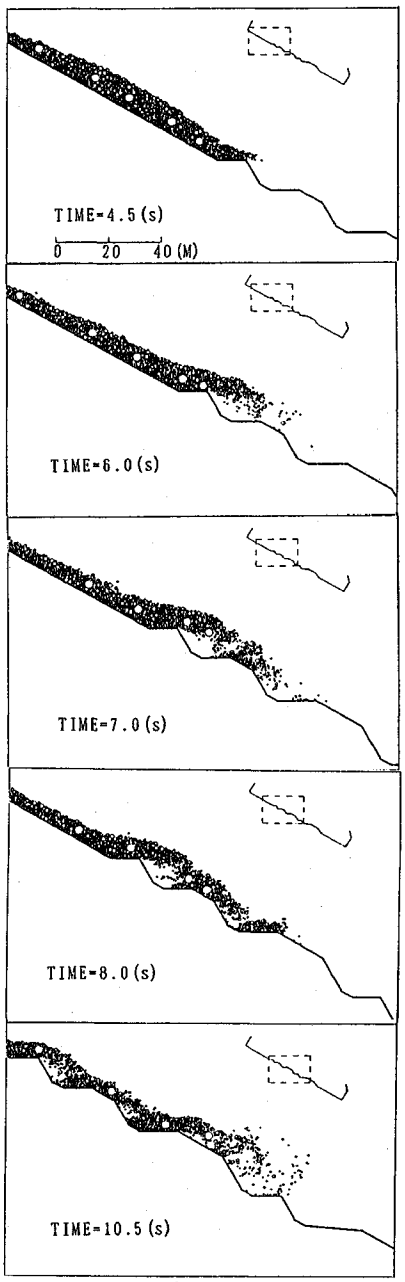

Fig.4 (a) Close-up of the debris flow with the water effect.

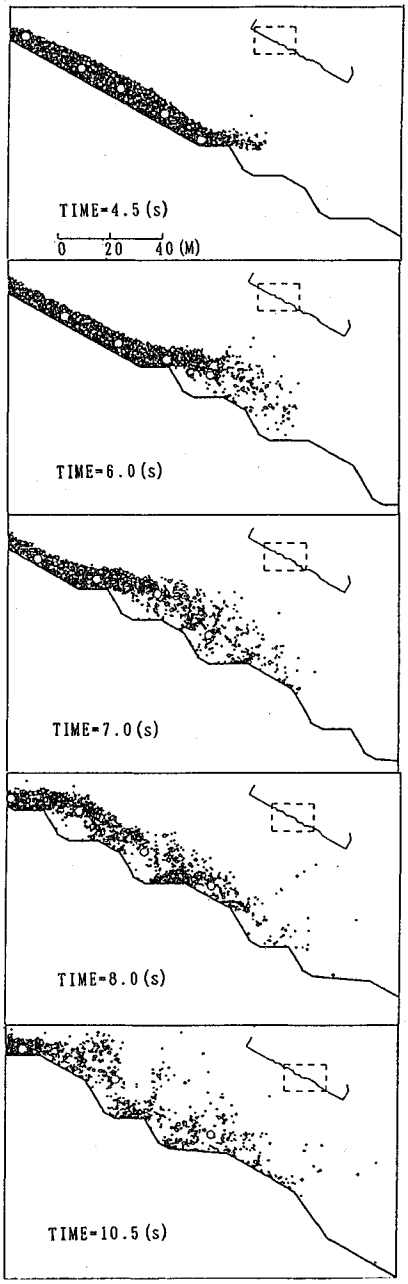

Fig.4 (b) Close-up of the dry avalanche simulation for the compacted assembly and rough slope.

viscosity is created between the cobble stones or between the cobbles and slope owing to the effect of water. With respect to velocity, a comparison of **Figs.7** and 8 for the same analysis time of 7.5 sec shows that **Fig.7** (debris flow) has much less disturbance, and its velocity vector is considered to express the stream line of the fluid. Results indicate that the line of velocity is not disturbed even if the analysis time is more than 13 sec; (**Fig.9**), 16 sec (**Fig.10**) and 19.5 sec (**Fig.11**). The maximum velocity is less for 19.5 sec than for 16 sec.

The mean velocities of the particles as a whole are compared for the debris flow and granular rock avalanche in **Fig.12**. Both lines are almost overlapping from 0 to 2 sec; thereafter, a mutual interference force acts between the granular substances with water as the medium in the case of

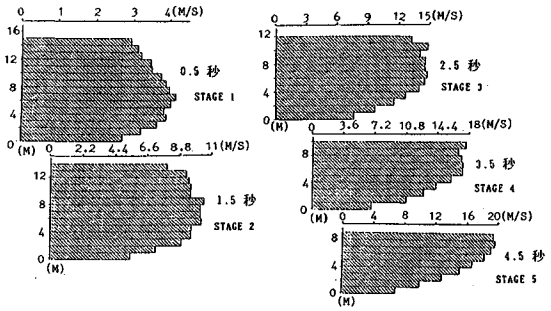

Fig.5 Flow velocity at various depths for debris flow with the water effect.

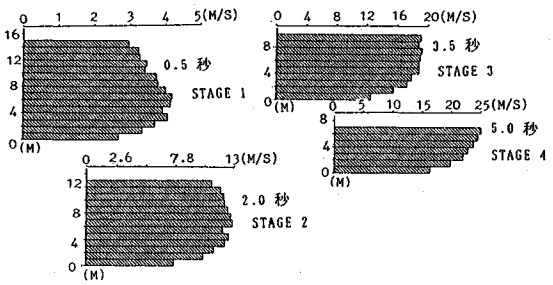

Fig.6 Flow velocity at various depth for a compacted dry avalanche.

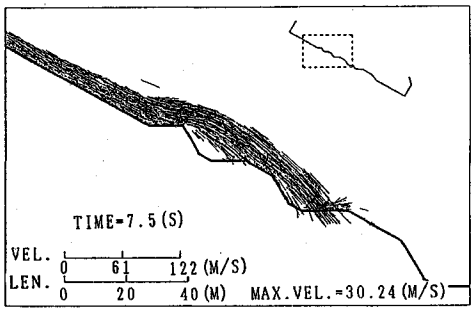

Fig.7 Velocity distribution 7.5 sec after the sliding of the debris flow with the water effect.

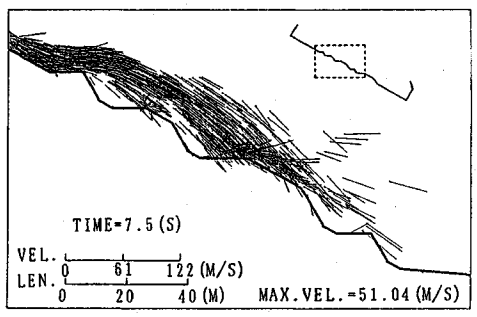

Fig.8 Velocity distribution 7.5 sec after the sliding of the compacted dry assembly.

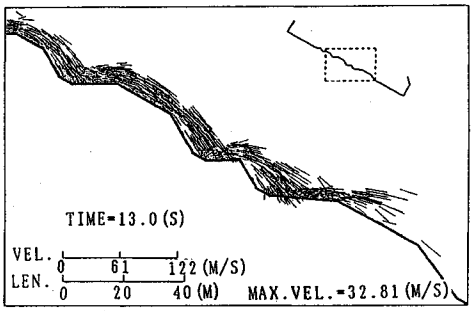

Fig.9 Velocity distribution 13.0 sec after sliding of debris flow with water effect.

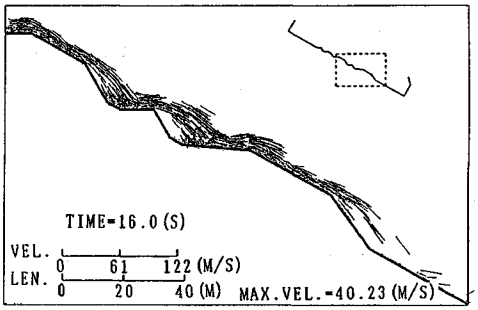

Fig.10 Velocity distribution 16.0 sec of the debris flow with the water effect.

the debris flow; and the mean velocity becomes slower than that of the granular rock avalanche. Moreover, the head portion has slowed down after 8 sec. The distributions of particles in both the debris flow and granular rock avalanche at the end of the analysis are shown in **Fig.13**.

4. IMPACT FORCE OF A DEBRIS FLOW ON A VERTICAL WALL

As the simulation of the debris flow was made by the DEM taking into account the effect of water, the degree of the impact force when a debris flow collides with a vertical wall such as an erosion control dam (sabo dam) was analyzed using the same flow. The slope used had a 60-m-high vertical wall inserted in the middle of the rough slope model used in the previous analysis. The calculated results for the previous debris flow were used up to 6.5 sec, after which was made the slope with the vertical wall attached was used.

The period of analysis was from 6.5 to 15 sec. The positions and velocities of particles are shown in **Fig.14**. The movement of the particles with time shows that the head portion of the debris flow moved down the slope and reached the retaining wall at 7 sec, at which time the particles began to accumulate there. The accumulating particles were pushed up and moved further upward along the wall by the arrival of subsequent particles, and

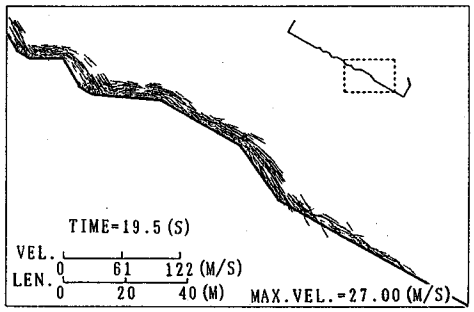

Fig.11 Velocity distribution 19.5 sec of the debris flow with the water effect.

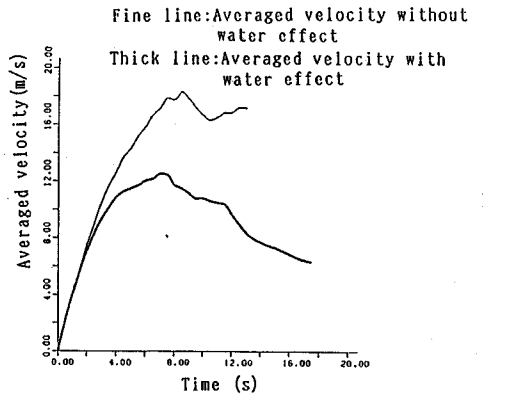

Fig.12 Average flow velocities for a dry avalanche and debris flow with water effect.

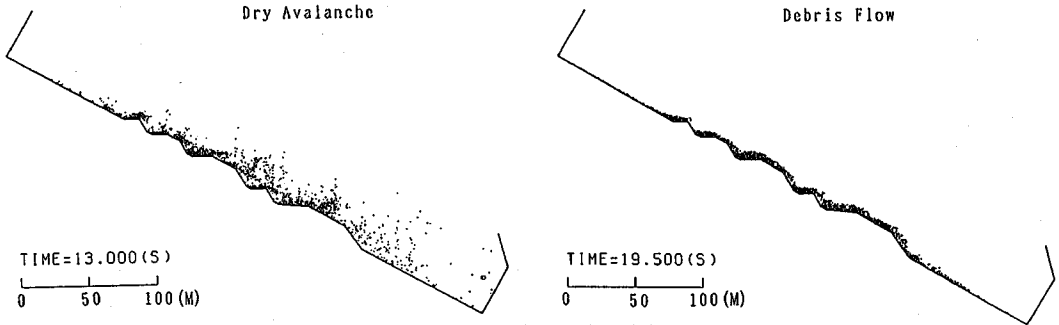

Fig.13 A dry avalanche and a debris flow.

these upper particles began to move in reverse to the incoming direction from 9 to 11 sec. At 12 sec, the upward moving the particles collided with particles coming from the slope. Thereafter, particles along the wall mostly lost velocity and piled up. This series of movements from the time of impact on the wall to deposition is very similar to that for a fluid; e.g., water. The flow backward along the wall and collision with the particles flowing from the slope, in particular, is very similar to the phenomenon of sea waves colliding with a breakwater.

The kinds of force giving impact to the wall by the debris flow are shown in **Figs.15~18**. **Figs.15** and **16** show the force vector applied to each wall element from 9 to 15 sec of the analysis. This force applied to the wall was followed throughout the analysis period (**Figs.17** and 18). **Fig.17** is a plot of the force applied to the wall in the lateral direction on the ordinate and the period of analysis is shown on the abscissa. **Fig.18** shows the bending moment about the root of the retaining wall is shown as the center on the ordinate, and the period of analysis is shown on the abscissa. Two kinds of forces exert pressure against the wall; the impact load that occurs when the particles collide with the wall, and the static pressure that occurs when the particles accumulate along the wall. The resultants of these forces are shown in **Figs.17** and 18. The first element in the analysis is the concentrated impact load; the force produced by the collision of the particles with the retaining wall. Its waveform consists of numerous pulses. Thereafter, another type of pressure is produced as a result of the deposition of particles along the wall, and the impact force on the wall is increased. The pressure waveform created by the deposition of the particles is considered to be smooth; therefore, the pressure that rapidly fluctuates vertically (**Figs.17** and 18) seems to be due to the impact load. In the final stage of the analysis, the waveform gradually has become steady because the particles deposited around the wall are aggregated and individual particles have less chance of direct collision with the wall; but, still fluctuates vertically which shows that other particles are still colliding with the deposited particles and that, as a result, the concentrated load propagates the impact force through the particles to the wall.

5. DEPOSITION PROCESS OF THE DEBRIS FLOW

Information on the debris flow on the rough slope was used for the first 6.5 sec. (as in Section

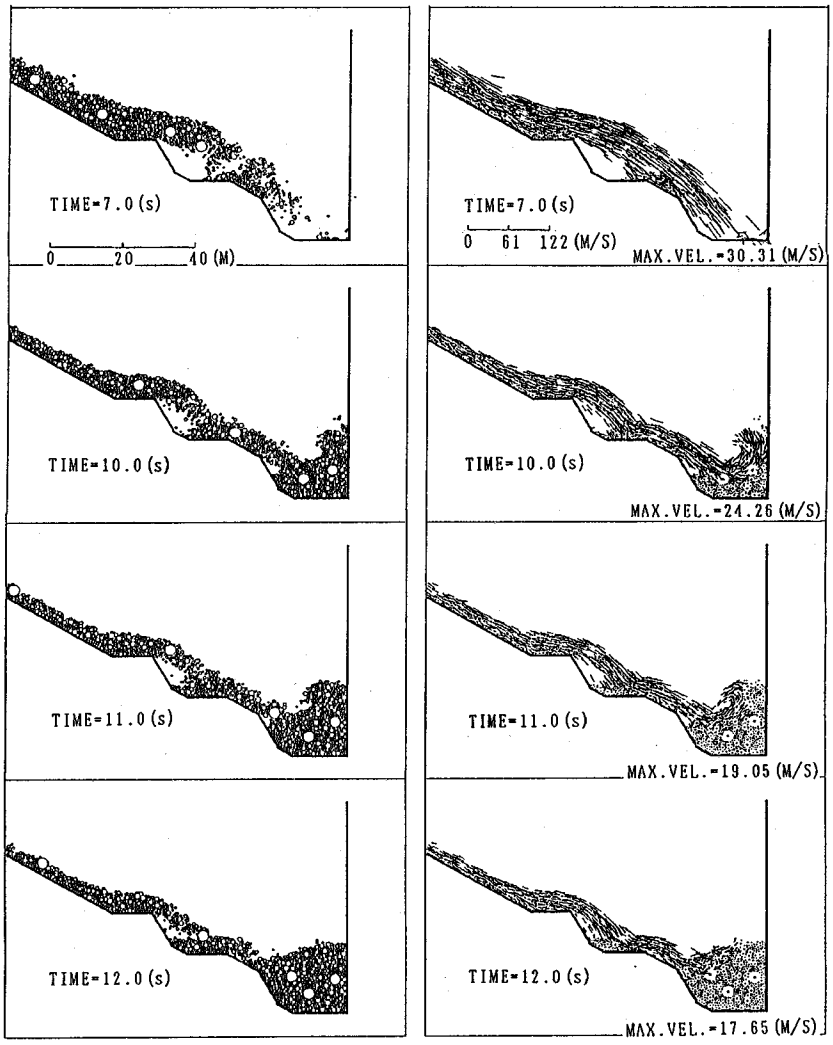

Fig.14 Impact of a debris flow on a wall.

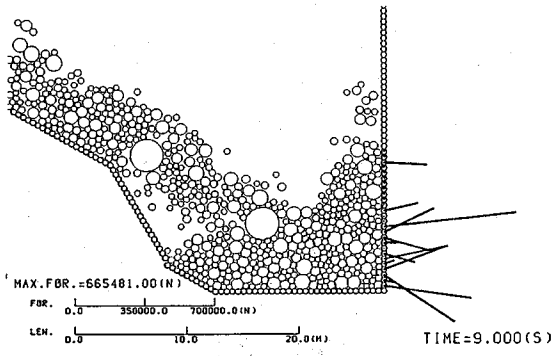

Fig.15 Impulsive force vectors on a wall due to a debris flow.

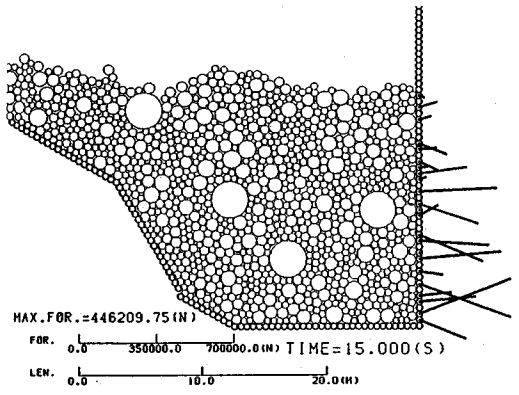

Fig.16 Impulsive force vectors on a wall due to a debris flow.

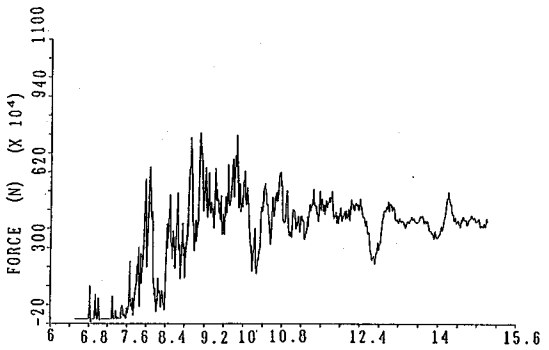

Fig.17 Total normal impulsive force on a wall caused by a debris flow.

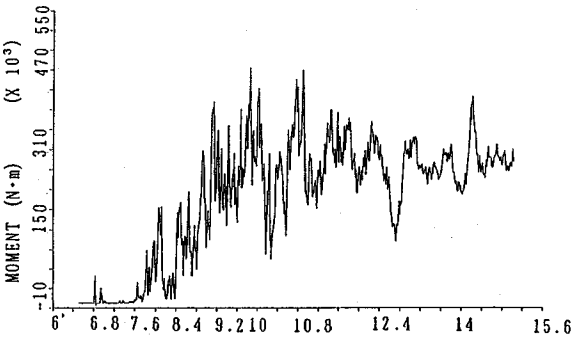

Fig.18 Total impulsive moment on a wall base caused by a debris flow.

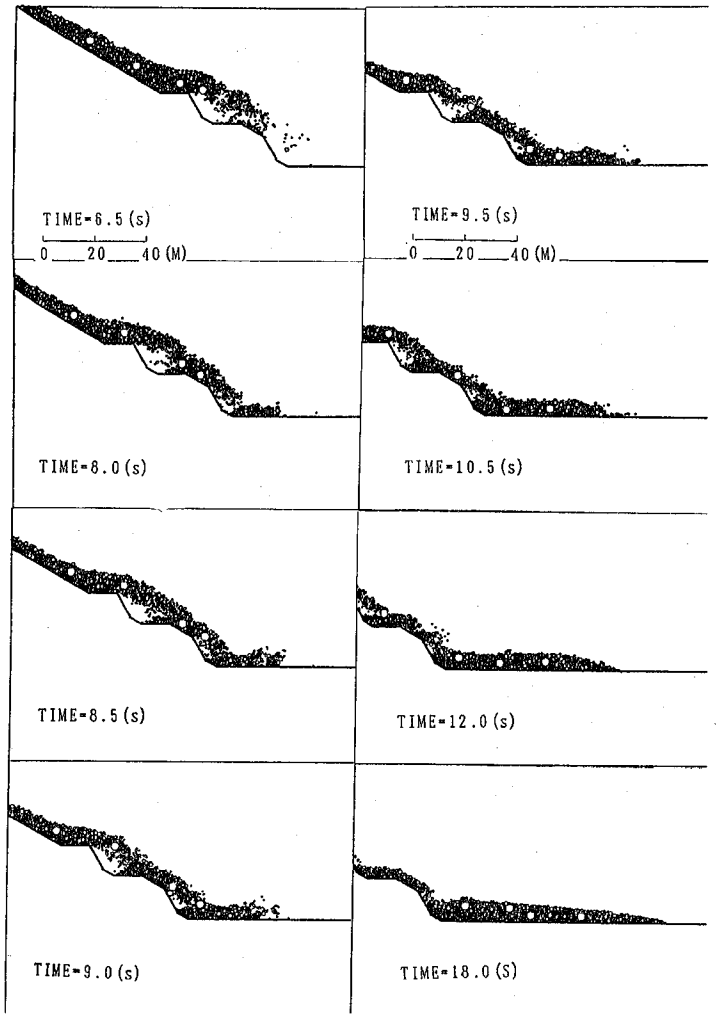

Fig.19 Deposition on process of the debris flow.

4), after which the flow on the horizontal plane was simulated. The period of analysis was from 6.5 to 18 sec. The particle distribution obtained as the result of the analysis is shown in **Fig.19**. Particles at the head portion of the flow bounce after colliding with the horizontal ground surface, producing a pattern that looks just like sea waves covering the top surface of a breakwater during a typhoon. This

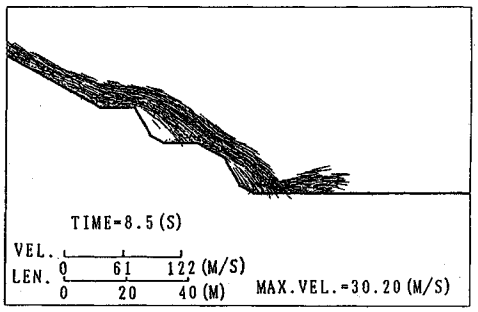

Fig.20 Particle velocity at 8.5 sec during sedimentation in a debris flow.

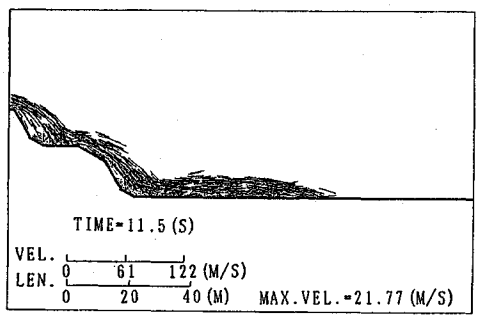

Fig.21 Particle velocity at 11.5 sec during sedimentation in debris flow.

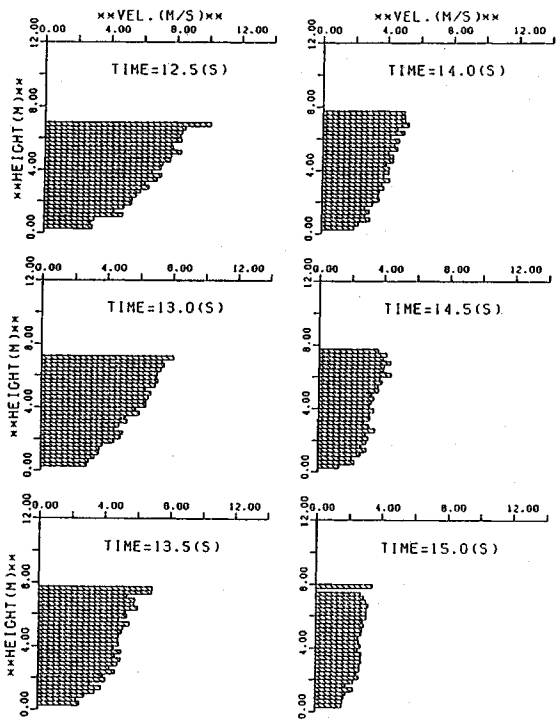

Fig.22 Velocity distribution at various heights from the bottom.

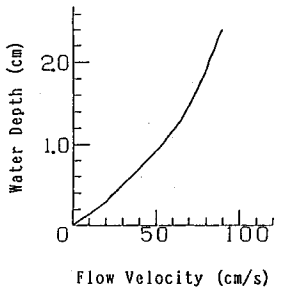

Fig.23 Theoretical velocity distribution of a debris flow.

situation also can be seen in **Fig.20** which shows the velocity diagram at 8.5 sec. But, after the scattered particles have collided with the ground several times, they become combined with the subsequent flow and begin to move as a mass again on the ground surface as indicated in the velocity diagram at 11.5 sec shown in **Fig.21**. Though not easily as understandable, **Fig.19** shows the head portion of this flow as a mass is an entraining phenomenon like a caterpillar between particles a phenomenon that also has been observed in granular rock avalanches. The velocity distribution at various heights was determined from the velocity of the particles moving parallel to the ground surface ; (**Fig.22**) ; these particles were two-thirds of the particles in the head portion of the flow entering the horizontal plane (if 90 particles entered the horizontal, 60 particles from the front were the sample). The shape from 12.5 to 13.5 sec is similar to that reported in fluid theory (**Fig.23**). As time elapses, the velocity decreases, the difference in speed between the points close to and far from the ground becomes smaller, and the velocity as a whole approaches 0 m/s. The velocity of each period of analysis (**Fig.22**) was averaged and plotted in **Fig.24** with the period of analysis on the abscissa. The values for the first several seconds are slightly disturbed because the number of particles considered was not sufficient. But, thereafter the mean velocity decreased as time elapsed and was almost 0 m/s at 18 sec.

The distribution and velocity of the particles at the end of analysis (18 sec) are shown in **Fig.25**. The deposited particles formed a mass that was 86.8 m long and of 10.7 m thick.

6. CONCENTRATION OF BOULDERS IN THE HEAD PORTION OF THE FLOW

The concentrating mechanism of boulders in the head portion of flow will be reviewed first. The orders of the particles with radii within a specified range (e.g., particles with a radius of 25 to 30 cm) which moved closer to the head portion of the flow between the initial state and the end of the analysis

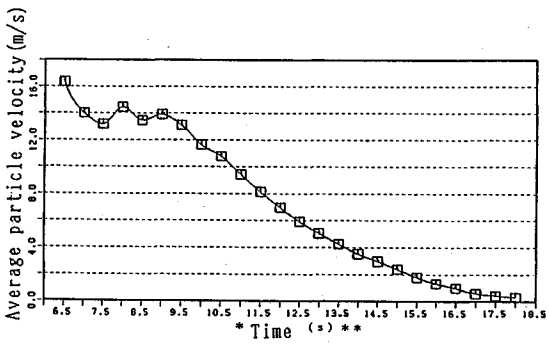

Fig.24 Averaged particle velocity versus Time.

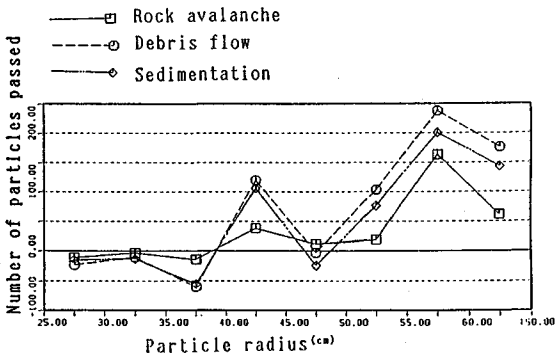

Fig.26 How many particles does a given particle pass.

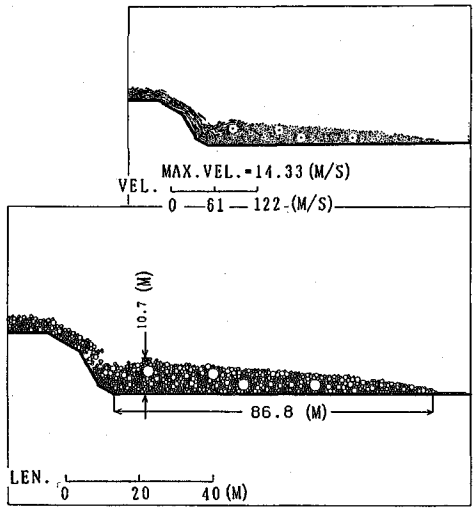

Fig.25 Particle and velocity distributions at 18.0 sec in debris flow.

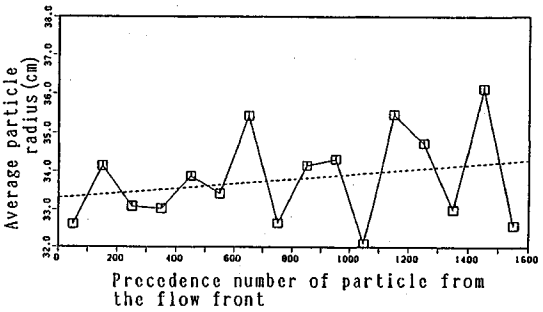

Fig.27 Particle radii distribution for the compacted model in the initial condition.

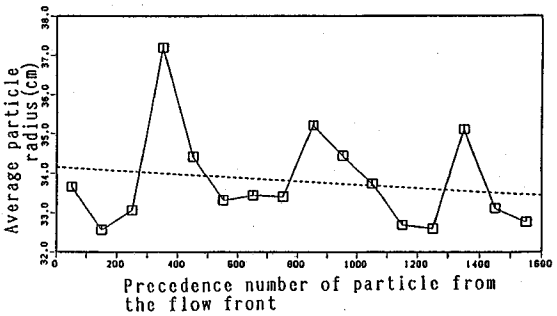

Fig.28 Particle radii distribution 13.0 sec in a dry rock avalanche.

are shown in **Fig.26**. The orders that moved closer to the head portion of the flow are plotted on the ordinate. The radii of the particles of three kinds of flows; a granular rock avalanche (rough slope), debris flow (rough slope) and debris flow (deposition process) are plotted on the abscissa. Similar patterns are seen in all three, in which particles with a larger radius obtain a higher order (closer to the head portion of the flow), this tendency being most marked in both types of debris flow.

The mean particle sizes of 100 particles counted from the heads of the flow for four situations 1) initial state, 2) at the end of the analysis of the granular rock avalanche (rough slope), 3) at the end of the analysis of the debris flow (rough slope) and 4) at the end of the analysis of the debris flow (deposition process) are shown in **Fig.27~30**. The dotted line in each figure is the regression straight line determined by the method of least squares. When this line slopes downward to the left, it means that particle size is smaller as particle location comes closer to the head of the flow. For the initial state shown in **Fig.27**, the straight regression line slopes downward to the left, but there is a marked distance between the line and each plotted point. This is the natural result of the random coordinate position and radius chosen for each particle in the initial stage. In the granular rock avalanche (rough slope) (**Fig.28**) the straight regression line slopes downward to the right, showing that particle size increases toward the head of the flow;but, as the distance from the straight line to each plotted point is relatively large, it connot be said that all particles of large size have

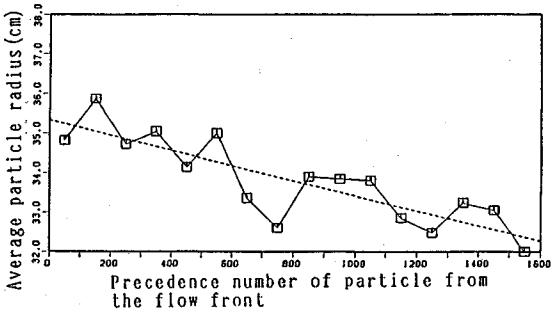

Fig.29 Particle radii distribution 19.5 sec in debris flow.

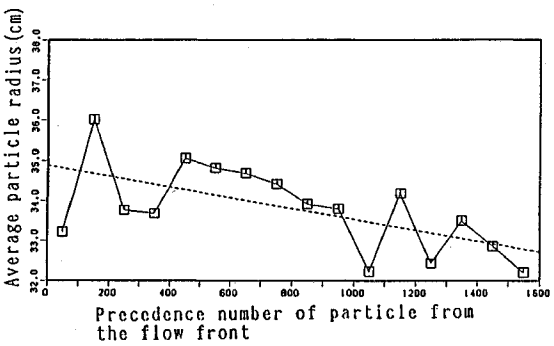

Fig.30 Particle radii distribution in deposition process at 18 sec.

moved to the head portion. In the case of the debris flow (rough slope) (**Fig.29**) the straight regression line slopes steeply to the right in comparison to the initial state. Each plotted point falls along this straight line, which means that the distribution of particle size within the flow from the initial state to the end of analysis has changed, particles of large size having moved toward the head portion of the flow. In **Fig.30** (deposition process), the straight regression line slopes downward to the right, but not as steeply as in the previous debris flow (slope). The straight regression lines from **Figs.27** to **30** are drawn together in **Fig.31**. Three cases indicate the tendency for particle size to become larger as particles are located closer to the head portion of a flow, and the debris flow (slope) has the steepest gradient. The models of granular rock avalanche (slope) and debris flow (slope) had the same internal elements and wall elements, the only the difference being whether the effect of water was considered in the DEM program.

All the calculations were done by a HITAC M280H (17 MIPS, 16 MB) in Earthquake Research Institute, University of Tokyo.

7. CONCLUSIONS

The following was demonstrated from our simulation of a debris flow using the Distinct

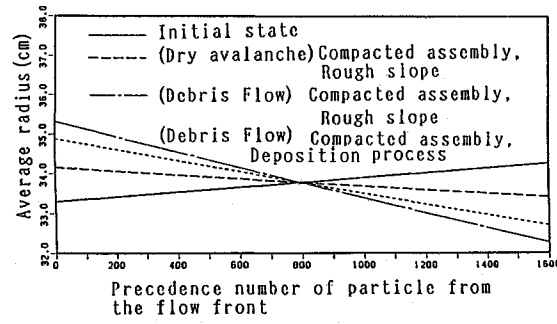

Fig.31 Particle radii distribution in cases of rock avalanche, debris flow.

Element Method:

(1) The concentration of boulders in the head portion of the flow could be determined by statistically pursuing each particle.

(2) The flow-down situation, as calculated taking into account the effect of water on a debris flow as a form of viscous resistance between particles is in good agreement with results of past observations.

(3) Compared to the dry granular rock avalanche, the debris flow had less velocity and less scattering even after passing through discontinuous points (e.g. rough up-and-down).

(4) Compared to the dry granular rock avalanche, the debris flow showed similarities to the flow of water, partly because the effect of water was taken into account.

(5) An entraining phenomenon similar to a caterpillar was recognized at the head portion of the flow.

(6) On collision with the vertical wall, a bouncing phenomenon similar to that seen in the collision of sea waves with a breakwater took place.

A debris flow is a multiphase flow comprised of solids such as stones and boulders as well as water. We simulated a debris flow using the Distinct Element Method (1) with emphasis on the analysis of solid granular matter with the mass of water neglected and by (2) adding a mutual interference term (viscous resistance) using water as the medium between the granular material. The results obtained gave an approximation of the real phenomena of a debris flow.

ACKNOWLEDGMENT: We are deeply grateful to Masahiro Isobe, Associate Professor of Civil Engineering Department, Faculty of Engineering, University of Tokyo for his advice and suggestions.

REFERENCES

1) Mogami, T.:A Statistical Approach of the Mechanics of Granular Materials, Soils and Foundations, Vol.5, No.2, pp.26-36, 1965.

2) Satake, M.:On Distortion of Tensor and Yield Criteria of Granular Materials, Int. J. Engineering Science, Vol.19, No.12, pp.1643-1650, 1981.
3) Cundall, P.A.:A Computer Model for Simulating Progressive, Large Scale Movement in Blocky Rock Systems, Symp. ISRM. Nancy, France, Proc.2, pp.129-136, 1971.
4) Cundall, P.A. and Strack, O.D.L.:A Discrete Numerical Model for Granular Assemblies, Geotechnique, Vol.2, No.1, pp.47-65, 1979.
5) Uemura, D. and Hakuno, M.:Granular Assembly Simulation with Cundall's Model for the Dynamic Collapse of the Structural Foundation, Structural Eng./Earthquake Eng., Proc. of Japan Society of Civil Engineers, Vol.4, No.1, pp.155 s-164 s, 1987.
6) Hakuno, M. and Tarumi, Y.:A Granular Assembly Simulation for Seismic Liquefacion of Sand, Structural Eng./Earthquake Eng., Vol.5, No.2, pp.333 s-342 s, Proc. Japan Society of Civil Engineers, 1988.
7) Iwashita, K. and Hakuno, M.:Modified Distinct Element Method Simulation of Dynamic Cliff Collapse, Structural Eng./Earthquake Eng., Vol.7, No.1, pp.133 s-142 s, Proc. Japan Society of Civil Engineers, 1990.
8) Uchida, Y. and Hakuno, M.:Distinct Element Analysis of Dry Rock Avalanches, Structural Eng./Earthquake Eng., Vol.7, No.2, pp.206 s-214 s, Proc. Japan Society of Civil Engineers, 1990.

(Received October 2, 1989)

土石流の個別要素法解析

伯野元彦・内田吉彦

土石流は降雨のみにより発生する以外にも，地震後の山腹崩壊が河川と合流し，土石流となったり，噴火でも，水の供給が少なければ火砕流となったり，多ければ土石流となったりする．今回は，土石流中の石は円板要素で近似し，水の影響は，要素間の相対速度の2乗に比例する抵抗という簡単な仮定でシミュレーション解析を行った．その結果，流れ方は乾燥岩屑流と比較して水の流れ方に近づき，流速は遅く，飛散は少なくなった．また，凹凸のある斜面を流下しているうちに，大粒子が流れの前方に移動する傾向のあることも知られ，砂防ダムのような鉛直壁と衝突したときの挙動も解析した．